Can we simulate the quantum dynamics of many electrons both, accurately and fast?

Michael Bonitz, Niclas Schlünzen, Jan-Philip Joost, Karsten Balzer, Lotte Borkowski, Hannes Ohldag, and Christopher Makait

in collaboration with Iva Brezinova, TU Vienna

C | A | U

Christian-Albrechts-Universität zu Kiel

Mathematisch-Naturwissenschaftliche Fakultät

U Michigan

Quantum Chemistry / Condensed Matter

Seminar October 2021

Finite correlated quantum systems

Fermionic atoms in optical lattices

tunable lattice depth and interaction

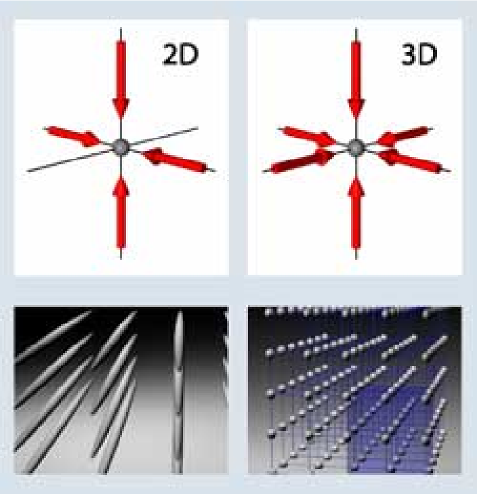

Fig.: M. Greiner (Harvard)

Graphene: high mobility, no bandgap

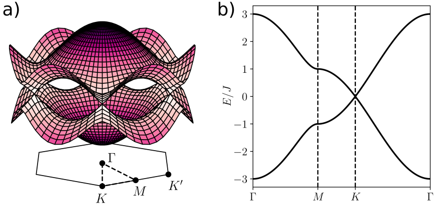

Graphene nanoribbons:

finite tunable bandgap

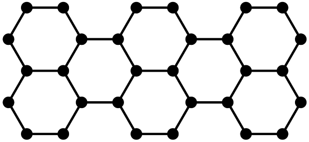

GNR: spatially localized spectral contributions[1]

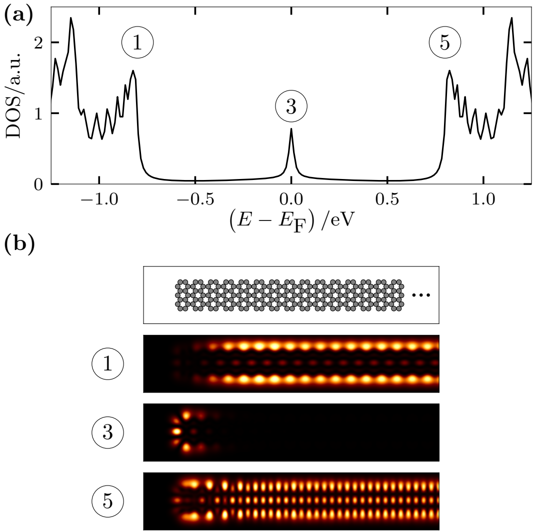

- top: total density of states (DOS)

- DOS size and shape dependent
- many degrees of freedom: combination of materials, multiple layers

- importance of e-e interactions
- what will happen in nonequilibrium, upon external excitation (e.g. by lasers)?

[1] 7 armchair GNR of 504 atoms, GW-NEGF ground state simulation, J.-P. Joost, A.-P. Jauho, and M. Bonitz, Nano Letters **19**, 9045 (2019)

Cold atoms in optical lattices: quench induced dynamics

- Prepare cold atoms at a given coupling strength U
- "Instantly" change the system parameters
- Observe the many-particle dynamics
- Question: how does the interaction strength influence the dynamics?

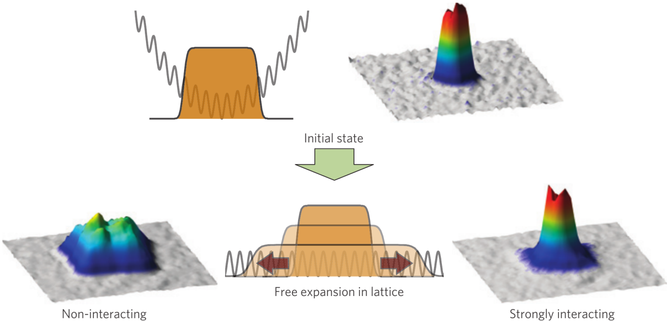

Diffusion of cold fermionic atoms following a confinement quench

[1] Schneider et al., Nature Phys. (2012).

Time-dependent Schrödinger equation. Scaling bottleneck

- time-dependent many-electron Hamiltonian

$$H(t) = \underbrace{\sum_{i=1}^{N} h(\boldsymbol{r}_i, t)}_{\text{one-body operators}} + \underbrace{\frac{1}{2}\sum_{i\neq j}^{N} W(\boldsymbol{r}_i, \boldsymbol{r}_j)}_{\textbf{pair-wise}\text{ interactions}}$$

- time-dependent Schrödinger equation (TDSE)

$$i\partial_t \Psi(\boldsymbol{r}_i, \ldots, \boldsymbol{r}_N; t) = H(t)\Psi(\boldsymbol{r}_i, \ldots, \boldsymbol{r}_N; t) \quad \underset{\text{exponential scaling of numerical effort}}{\overset{\text{direct solution}}{\not\Longrightarrow}} \quad \Psi(\boldsymbol{r}_i, \ldots, \boldsymbol{r}_N; t)$$

- **solutions to overcome exponential scaling:**
  1. approximations to TDSE: TD-RASCI, TD-CASSCF, truncated CC, TD-R-matrix etc. D. Hochstuhl and M. Bonitz, PRA (2012) and EJP-ST (2014), embedding techniques
  2. propagation of simpler observables: density (TDDFT), distribution function (Kinetic theory), correlation functions etc.

C|A|U Christian-Albrechts-Universität zu Kiel
Mathematisch-Naturwissenschaftliche Fakultät

- **Boltzmann's kinetic equation for the phase space distribution** $f(\mathbf{r}_1, \mathbf{p}_1, t)$

$$\frac{\partial f}{\partial t} + \frac{\mathbf{p}_1}{m} \cdot \nabla f + \mathbf{F}^{\text{tot}} \cdot \frac{\partial f}{\partial \mathbf{p}_1} = \int dp_2 dp_1' dp_2' \, \sigma(p_1, p_2; p_1', p_2') \left\{ f_1' f_2' - f_1 f_2 \right\} \Big|_t = I(p_1, t)$$

- I : two-particle scattering effects, modified by surrounding medium (e.g. screening)
- static screening: Landau; dynamic screening: Balescu-Lenard equation.

$$\sigma^{\text{BL}} \sim \left| \frac{V(p_1 - p_1')}{\epsilon\left(p_1 - p_1', E_{p_1} - E_{p_1'}\right)} \right|^2 \delta(p_1 + p_2 - p_1' - p_2')\, \delta(E_{p_1} + E_{p_2} - E_{p_1'} - E_{p_2'})$$

- **Problems of the Boltzmann and Balescu equations:**[2]
  1. neglect of strong coupling/multiple scattering effects (T-matrix diagrams)
  2. no total energy conservation
  3. not applicable to femtosecond time scales (no correlation buildup)

[2] for details, see M. Bonitz, *Quantum Kinetic Theory*, 2nd ed., Springer 2016

Scaling of quantum many-body methods

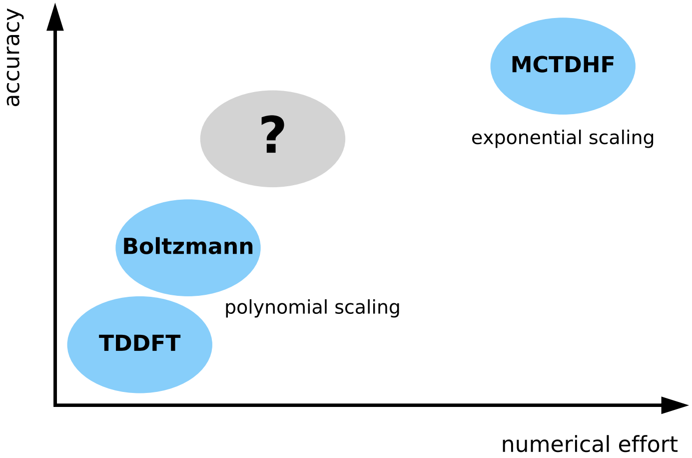

*MCTDHF and other wavefunction-based methods

? Can one achieve sufficient accuracy (including e-e correlations) at non-exponential cost?

2nd quantization

- Fock space $\mathcal{F} \ni |n_1, n_2 \ldots\rangle$, $\quad \mathcal{F} = \bigoplus_{N_0 \in \mathbb{N}} \mathcal{F}^{N_0}$, $\quad \mathcal{F}^{N_0} \subset \mathcal{H}^{N_0}$
- $\hat{c}_i$,$\hat{c}_i^\dagger$ creates/annihilates a particle in single-particle orbital ϕ_i
- spin accounted for by canonical (anti-)commutator relations
$$\left[\hat{c}_i^{(\dagger)},\, \hat{c}_j^{(\dagger)}\right]_\mp = 0, \qquad \left[\hat{c}_i,\, \hat{c}_j^\dagger\right]_\mp = \delta_{i,j}$$
- Hamiltonian: $\hat{H}(t) = \underbrace{\sum_{k,m} h^0_{km} \hat{c}_k^\dagger \hat{c}_m}_{\hat{H}_0} + \underbrace{\frac{1}{2} \sum_{k,l,m,n} w_{klmn}\, \hat{c}_k^\dagger \hat{c}_l^\dagger \hat{c}_n \hat{c}_m}_{\hat{W}} + \hat{F}(t)$

Particle interaction w_{klmn}

- Coulomb interaction
- electronic correlations

Time-dependent excitation $\hat{F}(t)$

- single-particle type
- em field, quench, particles

Nonequilibrium Green Functions (NEGF)

two times $z, z' \in \mathcal{C}$ ("Keldysh contour"), arbitrary one-particle basis $|\phi_i\rangle$

$$\boxed{G_{ij}(z,z') = \frac{\mathrm{i}}{\hbar}\left\langle \hat{T}_{\mathcal{C}}\hat{c}_i(z)\hat{c}_j^\dagger(z')\right\rangle}$$

average with $\hat{\rho}_N$

pure or mixed state

Keldysh–Kadanoff–Baym equations (KBE) on $\mathcal{C}$ (2×2 matrix):

$$\sum_k \left\{\mathrm{i}\hbar\frac{\partial}{\partial z}\delta_{ik} - h_{ik}(z)\right\} G_{kj}(z,z') = \delta_{\mathcal{C}}(z,z')\delta_{ij} - \mathrm{i}\hbar\sum_{klm}\int_{\mathcal{C}} \mathrm{d}\bar{z}\, w_{iklm}(z^+,\bar{z})G^{(2)}_{lmjk}(z,\bar{z};z',\bar{z}^+)$$

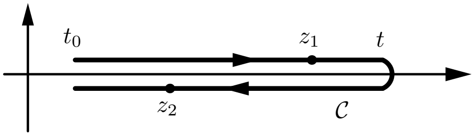

KBE: first equation of Martin–Schwinger hierarchy for $G, G^{(2)}\dots G^{(n)}$

- $\int_{\mathcal{C}} wG^{(2)} \to \int_{\mathcal{C}} \Sigma G$, Selfenergy
- Nonequilibrium Diagram technique
  Example: Hartree–Fock + Second Born selfenergy

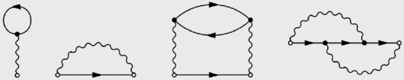

Real-Time Keldysh–Kadanoff–Baym Equations (KBE)

- Correlation functions $G^{\gtrless}$ obey real-time KBE

$$\sum_l \left[\mathrm{i}\hbar \frac{\mathrm{d}}{\mathrm{d}t}\delta_{i,l} - h^{\text{eff}}_{il}(t)\right] G^{>}_{lj}(t,t') = I^{(1),>}_{ij}(t,t')\,,$$

$$\sum_l G^{<}_{il}(t,t')\left[-\mathrm{i}\hbar \frac{\overleftarrow{\mathrm{d}}}{\mathrm{d}t'}\delta_{l,j} - h^{\text{eff}}_{lj}(t')\right] = I^{(2),<}_{ij}(t,t')\,,$$

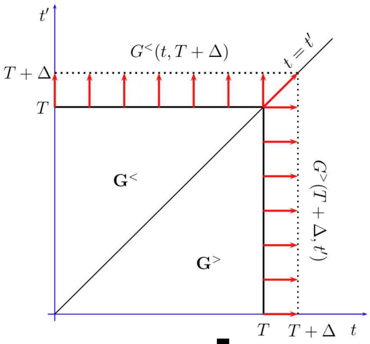

with the effective single-particle **Hartree–Fock Hamiltonian**

$$h^{\text{eff}}_{ij}(t) = h^0_{ij} \pm \mathrm{i}\hbar \sum_{kl} w^{\pm}_{ikjl} G^{<}_{lk}(t)$$

and the collision integrals

$$I^{(1),>}_{ij}(t,t') := \sum_l \int_{t_\text{s}}^{\infty} \mathrm{d}\bar{t}\left\{\Sigma^{\text{R}}_{il}(t,\bar{t})G^{>}_{lj}(\bar{t},t') + \Sigma^{>}_{il}(t,\bar{t})G^{\text{A}}_{lj}(\bar{t},t')\right\},$$

$$I^{(2),<}_{ij}(t,t') := \sum_l \int_{t_\text{s}}^{\infty} \mathrm{d}\bar{t}\left\{G^{\text{R}}_{il}(t,\bar{t})\Sigma^{<}_{lj}(\bar{t},t') + G^{<}_{il}(t,\bar{t})\Sigma^{\text{A}}_{lj}(\bar{t},t')\right\}.$$

$$\mathcal{O}(N_\text{t}^3)$$

- two-time structure contains spectral information
- numerically demanding due to cubic scaling with number of time steps N_t

Selfenergy Approximations[3]

Hartree–Fock (HF, mean field): $\sim w^1$

Second Born (2B): $\sim w^2$

GW: ∞ bubble summation,
dynamical screening effects

particle-particle T-matrix (TPP):
∞ ladder sum in pp channel

particle-hole T-matrix (TPH/TEH):
∞ ladder sum in ph channel

3rd order approx. (TOA): $\sim w^3$

dynamically screened ladder (DSL)*:
$\sim \mathrm{2B} + GW + \mathrm{TPP} + \mathrm{TPH}$

Choice depends on coupling strength, density (filling)

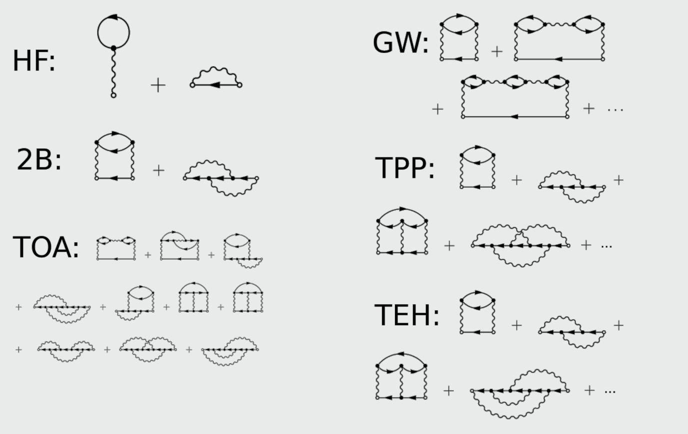

[3] Conserving approximations, nonequilibrium $\Sigma(t, t')$, applies for ultra-short to long times
Review: Schlünzen *et al.*, J. Phys. Cond. Matt. **32**, 103001 (2020); *Joost *et al.*, PRB (2022)

Testing various selfenergies: the Hubbard model

- Simple, but versatile model for strongly correlated solid state systems
- Suitable for single band, small bandwidth

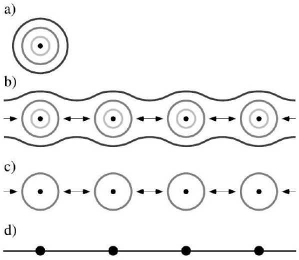

$\Rightarrow$

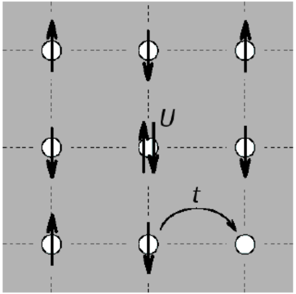

$$\boxed{\hat{H}(t) = J\sum_{ij,\,\alpha} h_{ij}\,\hat{c}^\dagger_{i\alpha}\hat{c}_{j\alpha} + U\sum_i \hat{c}^\dagger_{i\uparrow}\hat{c}_{i\uparrow}\hat{c}^\dagger_{i\downarrow}\hat{c}_{i\downarrow} + \sum_{ij,\alpha\beta} f_{ij,\alpha\beta}(t)\,\hat{c}^\dagger_{i\alpha}\hat{c}_{j\beta}}$$

$h_{ij} = -\delta_{\langle i,\,j\rangle}$ and $\delta_{\langle i,\,j\rangle} = 1$, if (i,j) is nearest neighbor, $\delta_{\langle i,\,j\rangle} = 0$ otherwise
use $J = 1$, on-site repulsion $(U > 0)$ or attraction $(U < 0)$, tunable interaction strength

Benchmarks of NEGF against DMRG (1D)[4]

Initial state:

charge density wave

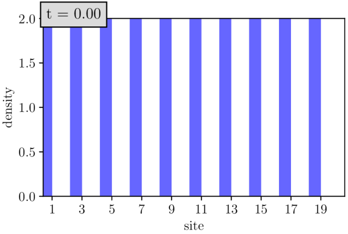

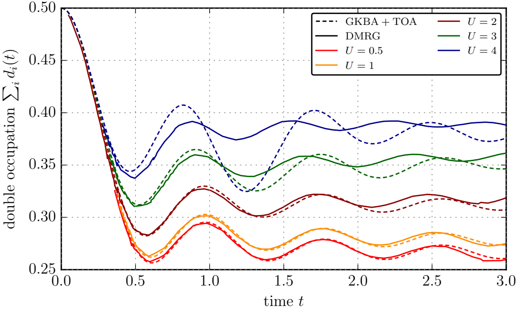

- sensitive observable: total double occupation
- good quality transients NEGF up to $U \simeq$ bandwidth
- Accurate long-time behavior of GKBA+T-matrix (not shown)

[4] N. Schlünzen, J.-P. Joost, F. Heidrich-Meisner, and M. Bonitz, Phys. Rev. B **95**, 165139 (2017)

Core expansion velocity: NEGF result[5] vs. experiment and RTA[6]

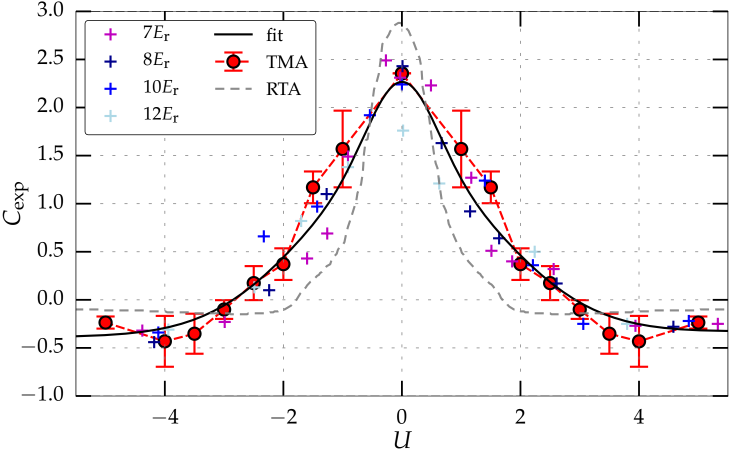

- Many-fermion expansion following sudden removal of confinement: interaction effects
- agreement with measurements for the *final stage* of the dynamics
- in addition: NEGF predict early stages, correlation dynamics etc.

---

[5] N. Schlünzen, S. Hermanns, M. Bonitz, and C. Verdozzi, Phys. Rev. B **93**, 035107 (2016)

[6] U. Schneider *et al.*, Nature Physics **8**, 213-218 (2012)

Acceleration: Generalized Kadanoff–Baym Ansatz (GKBA)[7]

- full propagation on the time diagonal ($I := I^{(1),<}$):

$$\mathrm{i}\hbar\frac{\mathrm{d}}{\mathrm{d}t}G^{<}_{ij}(t) = \left[h^{\mathrm{HF}}, G^{<}\right]_{ij}(t) + \left[I + I^{\dagger}\right]_{ij}(t)$$

- reconstruct off-diagonal NEGF from time diagonal:

$$G^{\gtrless}_{ij}(t,t') = \pm\left[G^{\mathrm{R}}_{ik}(t,t')\rho^{\gtrless}_{kj}(t') - \rho^{\gtrless}_{ik}(t)G^{\mathrm{A}}_{kj}(t,t')\right]$$

$$\text{with}\quad \rho^{\gtrless}_{ij}(t) = \pm\mathrm{i}\hbar G^{\lessgtr}_{ij}(t,t)$$

- HF-GKBA: use Hartree–Fock propagators for $G^{\mathrm{R/A}}_{ij}$

$$G^{\mathrm{R/A}}_{ij}(t,t') = \mp\mathrm{i}\Theta_{\mathcal{C}}\left(\pm[t-t']\right)\exp\left(-\frac{\mathrm{i}}{\hbar}\int_{t'}^{t}\mathrm{d}\bar{t}\,h_{\mathrm{HF}}(\bar{t})\right)\Bigg|_{ij}$$

- conserves total energy

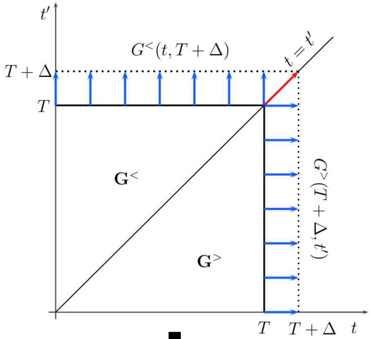

$$\mathcal{O}(N_{\mathrm{t}}^{2})$$

---

[6] P. Lipavský, V. Špička, and B. Velický, Phys. Rev. B **34**, 6933 (1986); K. Balzer and M. Bonitz, Lecture Notes in Physics **867** (2013)

GKBA results for materials, plasmas

C | A | U
Christian-Albrechts-Universität zu Kiel
Mathematisch-Naturwissenschaftliche Fakultät

2D Layered Materials

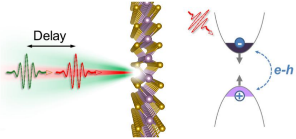

E. A. Pogna *et al.*,
ACS Nano **10**, 1182 (2016)

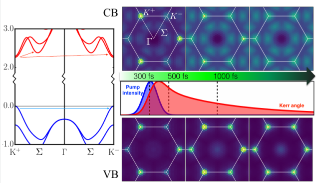

A. Molina-Sánchez *et al.*,
Nano Lett. **17**, 4549 (2017)

Ion Stopping in Hexagonal Lattices

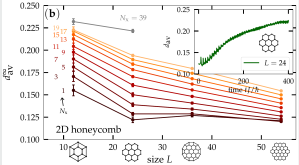

K. Balzer *et al.*,
PRL **121**, 267602 (2018)

Semiconductors

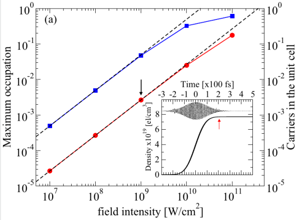

D. Sangalli *et al.*,
PRB **93**, 195205 (2016)

Laser-Induced Heating of Dense Plasmas

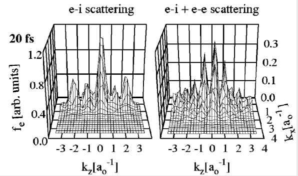

H. Haberland *et al.*,

PRE **64**, 026405 (2001)
gauge-invariant

multi-photon absorption

inv bremsstrahlung heating

GKBA results for atoms and molecules

Atoms

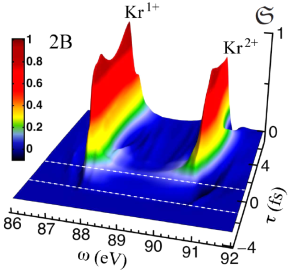

E. Perfetto *et al.*, PRA **92**, 033419 (2015)

Cold Atoms in Optical Lattices

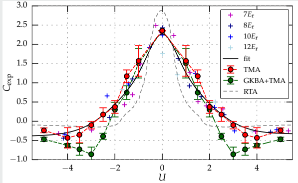

N. Schlünzen, M. Bonitz, CPP **56**, 5 (2016)

Σ beyond 2nd order

Biologically Relevant Molecules

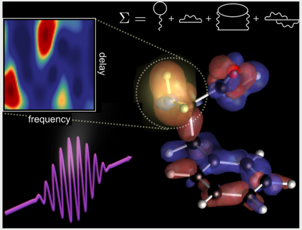

E. Perfetto *et al.*, JCPL **9**, 1353 (2018)

Carbon Allotropes

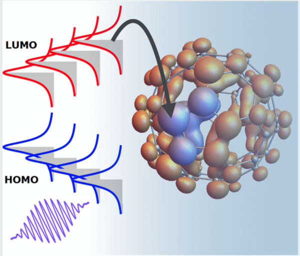

E. V. Boström *et al.*, Nano Lett. **18**, 785 (2018)

GKBA results for atoms and molecules

Atoms

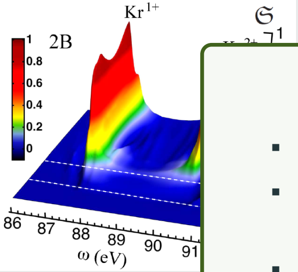

Cold Atoms in Optica

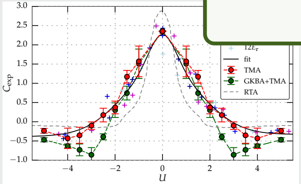

N. Schlünzen, M. Bonitz, CPP **56**, 5 (2016)

Σ beyond 2nd order

Biologically Relevant Molecules

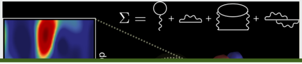

etto *et al.*,

), 1353 (2018)

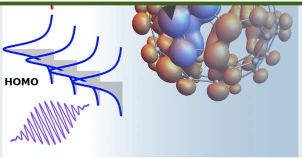

E. V. Boström *et al.*, Nano Lett. **18**, 785 (2018)

but

- improvement to N_t^2 scaling only possible for 2B selfenergy
- typical systems with small $N_b \sim 10–100$ but large $N_t \sim 1000–10000$
- still huge numerical disadvantage compared to other linearly scaling methods (TD-DMRG, TDDFT, TDSE)

Is $\mathcal{O}(N_t^1)$ scaling possible?

Reformulating the GKBA

- quadratic/cubic scaling is caused by the structure of the collision integral

$$I_{ij}(t) = \sum_k \underbrace{\int_{t_0}^{t} \mathrm{d}\bar{t}}_{\text{time integral}} \left[\Sigma^{>}_{ik}\boxed{(t,\bar{t})}G^{<}_{kj}\boxed{(\bar{t},t)} - \Sigma^{<}_{ik}\boxed{(t,\bar{t})}G^{>}_{kj}\boxed{(\bar{t},t)}\right]$$

time integral off-diagonal functions

Reformulating the GKBA

C | A | U
Christian-Albrechts-Universität zu Kiel
Mathematisch-Naturwissenschaftliche Fakultät

- quadratic/cubic scaling is caused by the structure of the collision integral

$$I_{ij}(t) = \sum_k \underbrace{\boxed{\int_{t_0}^{t} \mathrm{d}\bar{t}}}_{\text{time integral}} \left[\Sigma^{>}_{ik}\boxed{(t,\bar{t})} G^{<}_{kj}\boxed{(\bar{t},t)} - \Sigma^{<}_{ik}\boxed{(t,\bar{t})} G^{>}_{kj}\boxed{(\bar{t},t)}\right] =: \pm \mathrm{i}\hbar \sum_{klp} w_{iklp}(t) \boxed{\mathcal{G}_{lpjk}(t)}$$

time integral off-diagonal functions

Idea: solve differential equation for $\mathcal{G}$ instead of time integral for I

Reformulating the GKBA

- quadratic/cubic scaling is caused by the structure of the collision integral

$$I_{ij}(t) = \sum_k \underbrace{\boxed{\int_{t_0}^{t} \mathrm{d}\bar{t}}}_{\text{time integral}} \left[\Sigma^{>}_{ik}\boxed{(t,\bar{t})} G^{<}_{kj}\boxed{(\bar{t},t)} - \Sigma^{<}_{ik}\boxed{(t,\bar{t})} G^{>}_{kj}\boxed{(\bar{t},t)}\right] =: \pm\mathrm{i}\hbar \sum_{klp} w_{iklp}(t)\boxed{\mathcal{G}_{lpjk}(t)}$$

off-diagonal functions

Idea: solve differential equation for $\mathcal{G}$ instead of time integral for I

- example for 2B selfenergy[8]

$$\Sigma^{\gtrless}_{ij}\left(t,t'\right) = \pm\left(\mathrm{i}\hbar\right)^2 \sum_{klpqrs} w_{iklp}\left(t\right) w^{\pm}_{qrjs}\left(t'\right) G^{\gtrless}_{lq}\left(t,t'\right) G^{\gtrless}_{pr}\left(t,t'\right) G^{\lessgtr}_{sk}\left(t',t\right)$$

- respective $\mathcal{G}$ can be identified as

$$\mathcal{G}_{ijkl}(t) = \mathrm{i}\hbar \sum_{pqrs} \int_{t_0}^{t} \mathrm{d}\bar{t}\, w^{\pm}_{pqrs}\left(\bar{t}\right) \left[\mathcal{G}^{\mathrm{H},>}_{ijpq}(t,\bar{t})\mathcal{G}^{\mathrm{H},<}_{rskl}(\bar{t},t) - \mathcal{G}^{\mathrm{H},<}_{ijpq}(t,\bar{t})\mathcal{G}^{\mathrm{H},>}_{rskl}(\bar{t},t)\right]$$

with the two-particle Hartree Green function

$$\mathcal{G}^{\mathrm{H},\gtrless}_{ijkl}(t,t') := G^{\gtrless}_{ik}(t,t')G^{\gtrless}_{jl}(t,t')$$

[8] N. Schlünzen, J.-P. Joost and M. Bonitz, Phys. Rev. Lett. **124**, 076601 (2020)

Reformulating the GKBA

- quadratic/cubic scaling is caused by the structure of the collision integral

$$I_{ij}(t) = \sum_k \underbrace{\boxed{\int_{t_0}^{t} \mathrm{d}\bar{t}}}_{\text{time integral}} \left[\Sigma^{>}_{ik}\boxed{(t,\bar{t})}G^{<}_{kj}\boxed{(\bar{t},t)} - \Sigma^{<}_{ik}\boxed{(t,\bar{t})}G^{>}_{kj}\boxed{(\bar{t},t)}\right] =: \pm\mathrm{i}\hbar \sum_{klp} w_{iklp}(t)\boxed{\mathcal{G}_{lpjk}(t)}$$

time integral off-diagonal functions **Idea:** solve differential equation for $\mathcal{G}$ instead of time integral for I

- example for 2B selfenergy[8]

$$\Sigma^{\gtrless}_{ij}\left(t,t'\right) = \pm\left(\mathrm{i}\hbar\right)^2 \sum_{klpqrs} w_{iklp}\left(t\right) w^{\pm}_{qrjs}\left(t'\right) G^{\gtrless}_{lq}\left(t,t'\right) G^{\gtrless}_{pr}\left(t,t'\right) G^{\lessgtr}_{sk}\left(t',t\right)$$

- respective $\mathcal{G}$ can be identified as

$$\boxed{\mathcal{G}_{ijkl}(t) = \mathrm{i}\hbar \sum_{pqrs} \int_{t_0}^{t} \mathrm{d}\bar{t}\, w^{\pm}_{pqrs}\left(\bar{t}\right) \left[\mathcal{G}^{\mathrm{H},>}_{ijpq}(t,\bar{t})\mathcal{G}^{\mathrm{H},<}_{rskl}(\bar{t},t) - \mathcal{G}^{\mathrm{H},<}_{ijpq}(t,\bar{t})\mathcal{G}^{\mathrm{H},>}_{rskl}(\bar{t},t)\right]}$$

with the two-particle Hartree Green function

$$\mathcal{G}^{\mathrm{H},\gtrless}_{ijkl}(t,t') := G^{\gtrless}_{ik}(t,t')G^{\gtrless}_{jl}(t,t')$$

[8] N. Schlünzen, J.-P. Joost and M. Bonitz, Phys. Rev. Lett. **124**, 076601 (2020)

Reformulating the GKBA

- two-particle $\mathcal{G}$ in GKBA

$$\mathcal{G}_{ijkl}(t) = (\mathrm{i}\hbar)^3 \sum_{pqrs} \int_{t_0}^{t} \mathrm{d}\bar{t}\, \mathcal{U}^{(2)}_{ijpq}(t,\bar{t}) \boxed{\Psi^{\pm}_{pqrs}(\bar{t})} \mathcal{U}^{(2)}_{rskl}(\bar{t},t)$$

with the single-time source term (which no longer depends on the outer time)

$$\boxed{\Psi^{\pm}_{ijkl}(t)} = (\mathrm{i}\hbar)^2 \sum_{pqrs} w^{\pm}_{pqrs}(t) \left[\mathcal{G}^{\mathrm{H},>}_{ijpq}(t,t) \mathcal{G}^{\mathrm{H},<}_{rskl}(t,t) - \mathcal{G}^{\mathrm{H},<}_{ijpq}(t,t) \mathcal{G}^{\mathrm{H},>}_{rskl}(t,t) \right]$$

and the two-particle Hartree–Fock time-evolution operators obeying Schrödinger-type EOMs

$$\frac{\mathrm{d}}{\mathrm{d}t} \left[\mathcal{U}^{(2)}_{ijkl}(t,\bar{t}) \right] = \frac{1}{\mathrm{i}\hbar} \sum_{pq} h^{(2),\mathrm{HF}}_{ijpq}(t) \mathcal{U}^{(2)}_{pqkl}(t,\bar{t})$$

$$\frac{\mathrm{d}}{\mathrm{d}t} \left[\mathcal{U}^{(2)}_{ijkl}(\bar{t},t) \right] = -\frac{1}{\mathrm{i}\hbar} \sum_{pq} \mathcal{U}^{(2)}_{ijpq}(\bar{t},t) h^{(2),\mathrm{HF}}_{pqkl}(t)$$

with the effective two-particle Hamiltonian

$$h^{(2),\mathrm{HF}}_{ijkl}(t) = \delta_{jl} h^{\mathrm{HF}}_{ik}(t) + \delta_{ik} h^{\mathrm{HF}}_{jl}(t)$$

Time-linear NEGF simulations: the G1–G2 Scheme

- full propagation on the time diagonal as for ordinary HF-GKBA:

$$\mathrm{i}\hbar \frac{\mathrm{d}}{\mathrm{d}t} G^<_{ij}(t) = \left[h^{\mathrm{HF}}, G^<\right]_{ij}(t) + \left[I + I^\dagger\right]_{ij}(t)$$

- but collision integral defined by correlated two-particle Green function

$$I_{ij}(t) = \pm \mathrm{i}\hbar \sum_{klp} w_{iklp}(t) \mathcal{G}_{lpjk}(t)$$

- which obeys an ordinary differential equation[9]

$$\mathrm{i}\hbar \frac{\mathrm{d}}{\mathrm{d}t} \mathcal{G}_{ijkl}(t) = \left[h^{(2),\mathsf{HF}}, \mathcal{G}\right]_{ijkl}(t) + \Psi^{\pm}_{ijkl}(t)$$

$$\mathcal{O}(N_{\mathsf{t}}^1)$$

[9] two-particle commutator: $[A, B]_{ijkl}(t) = \sum_{pq} \left[A_{ijpq}(t) B_{pqkl}(t) - B_{ijpq}(t) A_{pqkl}(t)\right]$

Time-linear NEGF simulations: the G1–G2 Scheme

- full propagation on the time diagonal as for ordinary HF-GKBA:

$$\mathrm{i}\hbar\frac{\mathrm{d}}{\mathrm{d}t}G^<_{ij}(t) = \left[h^{\mathrm{HF}}, G^<\right]_{ij}(t) + \left[I + I^\dagger\right]_{ij}(t)$$

- but collision integral defined by correlated two-particle Green function

$$I_{ij}(t) = \pm\mathrm{i}\hbar\sum_{klp} w_{iklp}(t)\mathcal{G}_{lpjk}(t)$$

- which obeys an ordinary differential equation[9]

$$\mathrm{i}\hbar\frac{\mathrm{d}}{\mathrm{d}t}\mathcal{G}_{ijkl}(t) = \left[h^{(2),\mathsf{HF}}, \mathcal{G}\right]_{ijkl}(t) + \Psi^\pm_{ijkl}(t)$$

$$\mathcal{O}(N_\mathsf{t}^1)$$

- the initial values

$$G^{0,<}_{ij} = \pm\frac{1}{\mathrm{i}\hbar}n_{ij}(t_0) =: \pm\frac{1}{\mathrm{i}\hbar}n^0_{ij}\,,$$

$$\mathcal{G}^0_{ijkl} = \frac{1}{(\mathrm{i}\hbar)^2}\left\{n^0_{ijkl} - n^0_{ik}n^0_{jl} \mp n^0_{il}n^0_{jk}\right\}\,,$$

determine the density and the pair correlations existing in the system at the initial time $t = t_0$

[9] two-particle commutator: $[A, B]_{ijkl}(t) = \sum_{pq}\left[A_{ijpq}(t)B_{pqkl}(t) - B_{ijpq}(t)A_{pqkl}(t)\right]$

The G1–G2 Scheme: beyond 2nd Born selfenergy

- other selfenergy approximations can be reformulated in the G1–G2 scheme in similar fashion:[10]

$$\mathrm{i}\hbar\frac{\mathrm{d}}{\mathrm{d}t}\mathcal{G}_{ijkl}(t) = \left[h^{(2),\mathsf{HF}}(t), \mathcal{G}(t)\right]_{ijkl} + \Psi^{\pm}_{ijkl}(t) + \underbrace{L_{ijkl}(t)}_{\mathsf{TPP}} + \underbrace{P_{ijkl}(t)}_{GW} \pm \underbrace{P_{jikl}(t)}_{\mathsf{TPH}}$$

$$L_{ijkl} := \sum_{pq}\left\{\mathfrak{h}^{L}_{ijpq}\mathcal{G}_{pqkl} - \mathcal{G}_{ijpq}\left[\mathfrak{h}^{L}_{klpq}\right]^*\right\}, \qquad \mathfrak{h}^{L}_{ijkl} := (\mathrm{i}\hbar)^2\sum_{pq}\left[\mathcal{G}^{\mathsf{H},>}_{ijpq} - \mathcal{G}^{\mathsf{H},<}_{ijpq}\right] w_{pqkl}\,,$$

$$P_{ijkl} := \sum_{pq}\left\{\mathfrak{h}^{\Pi}_{qjpl}\mathcal{G}_{piqk} - \mathcal{G}_{qjpl}\left[\mathfrak{h}^{\Pi}_{qkpi}\right]^*\right\}, \qquad \mathfrak{h}^{\Pi}_{ijkl} := \pm(\mathrm{i}\hbar)^2\sum_{pq} w^{\pm}_{qipk}\left[\mathcal{G}^{\mathsf{F},>}_{jplq} - \mathcal{G}^{\mathsf{F},<}_{jplq}\right]$$

and the Hartree/Fock (H/F) two-particle Green functions

$$\mathcal{G}^{\mathsf{H},\gtrless}_{ijkl}(t) := G^{\gtrless}_{ik}(t,t)G^{\gtrless}_{jl}(t,t)\,, \qquad \mathcal{G}^{\mathsf{F},\gtrless}_{ijkl}(t) := G^{\gtrless}_{il}(t,t)G^{\lessgtr}_{jk}(t,t)$$

- include TPP, GW and TPH terms simultaneously: dynamically-screened-ladder (DSL) approximation. Conserving, applicable to short times. No explicit selfenergy known.
- nonequilibrium generalization of ground state result (Bethe-Salpeter equation)

[10] J.-P. Joost, N. Schlünzen, and M. Bonitz, PRB **101**, 245101 (2020), Joost et al., PRB **105**, 165155 (2022);

Numerical Scaling of G1–G2 vs. Standard HF-GKBA

- linear time scaling outweights introduction of 4-dimensional two-particle Green function
  $\rightarrow$ new scheme an improvement in most cases of practical relevance

		Σ				
Basis	**HF-GKBA**	**2B**	***GW***	**TPP**	**TPH**	**DSL**
general	standard	$\mathcal{O}\left(N_\mathrm{b}^5 N_\mathrm{t}^2\right)$	$\mathcal{O}\left(N_\mathrm{b}^6 N_\mathrm{t}^3\right)$	$\mathcal{O}\left(N_\mathrm{b}^6 N_\mathrm{t}^3\right)$	$\mathcal{O}\left(N_\mathrm{b}^6 N_\mathrm{t}^3\right)$	–
	G1–G2	$\mathcal{O}\left(N_\mathrm{b}^5 N_\mathrm{t}^1\right)$	$\mathcal{O}\left(N_\mathrm{b}^6 N_\mathrm{t}^1\right)$	$\mathcal{O}\left(N_\mathrm{b}^6 N_\mathrm{t}^1\right)$	$\mathcal{O}\left(N_\mathrm{b}^6 N_\mathrm{t}^1\right)$	$\mathcal{O}\left(N_\mathrm{b}^6 N_\mathrm{t}^1\right)$
	speedup ratio	$\mathcal{O}\left(N_\mathrm{t}\right)$	$\mathcal{O}\left(N_\mathrm{t}^2\right)$	$\mathcal{O}\left(N_\mathrm{t}^2\right)$	$\mathcal{O}\left(N_\mathrm{t}^2\right)$	–
Hubbard	standard	$\mathcal{O}\left(N_\mathrm{b}^3 N_\mathrm{t}^2\right)$	$\mathcal{O}\left(N_\mathrm{b}^3 N_\mathrm{t}^3\right)$	$\mathcal{O}\left(N_\mathrm{b}^3 N_\mathrm{t}^3\right)$	$\mathcal{O}\left(N_\mathrm{b}^3 N_\mathrm{t}^3\right)$	–
	G1–G2	$\mathcal{O}\left(N_\mathrm{b}^4 N_\mathrm{t}^1\right)$	$\mathcal{O}\left(N_\mathrm{b}^4 N_\mathrm{t}^1\right)$	$\mathcal{O}\left(N_\mathrm{b}^4 N_\mathrm{t}^1\right)$	$\mathcal{O}\left(N_\mathrm{b}^4 N_\mathrm{t}^1\right)$	$\mathcal{O}\left(N_\mathrm{b}^4 N_\mathrm{t}^1\right)$
	speedup ratio	$\mathcal{O}\left(N_\mathrm{t}/N_\mathrm{b}\right)$	$\mathcal{O}\left(N_\mathrm{t}^2/N_\mathrm{b}\right)$	$\mathcal{O}\left(N_\mathrm{t}^2/N_\mathrm{b}\right)$	$\mathcal{O}\left(N_\mathrm{t}^2/N_\mathrm{b}\right)$	–
HEG	standard	$\mathcal{O}\left(N_\mathrm{b}^3 N_\mathrm{t}^2\right)$	$\mathcal{O}\left(N_\mathrm{b}^3 N_\mathrm{t}^3\right)$	$\mathcal{O}\left(N_\mathrm{b}^3 N_\mathrm{t}^3\right)$	$\mathcal{O}\left(N_\mathrm{b}^3 N_\mathrm{t}^3\right)$	–
	G1–G2	$\mathcal{O}\left(N_\mathrm{b}^3 N_\mathrm{t}^1\right)$	$\mathcal{O}\left(N_\mathrm{b}^3 N_\mathrm{t}^1\right)$	$\mathcal{O}\left(N_\mathrm{b}^4 N_\mathrm{t}^1\right)$	$\mathcal{O}\left(N_\mathrm{b}^4 N_\mathrm{t}^1\right)$	$\mathcal{O}\left(N_\mathrm{b}^4 N_\mathrm{t}^1\right)$
	speedup ratio	$\mathcal{O}\left(N_\mathrm{t}\right)$	$\mathcal{O}\left(N_\mathrm{t}^2\right)$	$\mathcal{O}\left(N_\mathrm{t}^2/N_\mathrm{b}\right)$	$\mathcal{O}\left(N_\mathrm{t}^2/N_\mathrm{b}\right)$	–

Numerical Scaling of G1–G2 vs. Standard HF-GKBA

- time-linear scaling achieved quickly for all approximations. Example: 10-site Hubbard chain

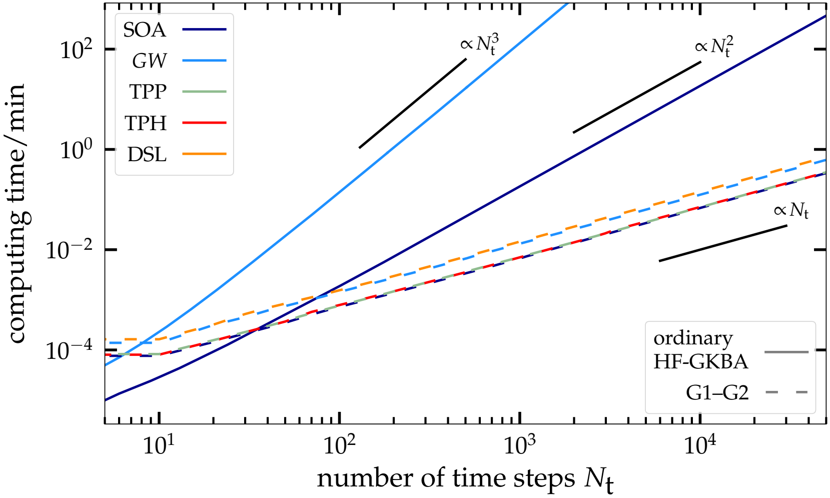

Numerical G1–G2 results: TPP vs. DSL

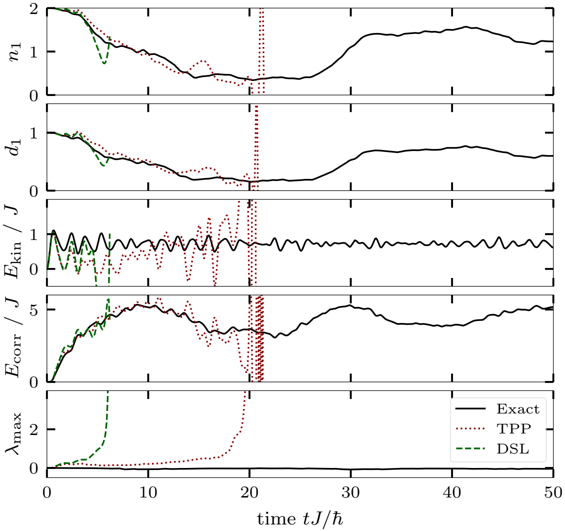

Figure 1: G1–G2 simulation for half-filled 6-site Hubbard system at moderate coupling, $U/J = 4$. Sites 1–3 are initially doubly occupied and sites 4–6 are empty. At time $t = 0$ the confinement potential is removed (quench). Instability for increasing U

G1–G2 scheme: achieving long simulation times for correlated electrons: contraction consistency and purification

- Enforcing Contraction consistency[11]:

$$\frac{N}{2} G_{ij}^{\uparrow\uparrow} = -\mathrm{i}\hbar \sum_p G_{ipjp}^{(2),\uparrow\downarrow\uparrow\downarrow}$$

$$G_{ij}^{\uparrow\uparrow} = -\mathrm{i}\hbar \sum_p G_{ippj}^{(2),\uparrow\downarrow\uparrow\downarrow}$$

$$\left(\frac{N}{2} - 1\right) G_{ijkl}^{(2),\uparrow\downarrow\uparrow\downarrow} = -\mathrm{i}\hbar \sum_p G_{ipjkpl}^{(3),\uparrow\uparrow\downarrow\uparrow\uparrow\downarrow}$$

$$\frac{N}{2} G_{ijkl}^{(2),\uparrow\uparrow\uparrow\uparrow} = -\mathrm{i}\hbar \sum_p G_{ijpklp}^{(3),\uparrow\uparrow\downarrow\uparrow\uparrow\downarrow}$$

$$G_{ijkl}^{(2),\uparrow\uparrow\uparrow\uparrow} = -\mathrm{i}\hbar \sum_p G_{ipjklp}^{(3),\uparrow\uparrow\downarrow\uparrow\uparrow\downarrow}$$

$$G_{ijkl}^{(2),\uparrow\uparrow\uparrow\uparrow} = -\mathrm{i}\hbar \sum_p G_{ijpkpl}^{(3),\uparrow\uparrow\downarrow\uparrow\uparrow\downarrow}$$

[11] see e.g. papers by Coleman, Maziotti and others
F. Lackner *et al.*, Phys. Rev. A (2015), Phys. Rev. A (2017)
J-P. Joost, N. Schlünzen, H. Ohldag, M. Bonitz, F. Lackner, and I. Brezinova, PRB (2022)

G1–G2 scheme: contraction consistency and purification[12]

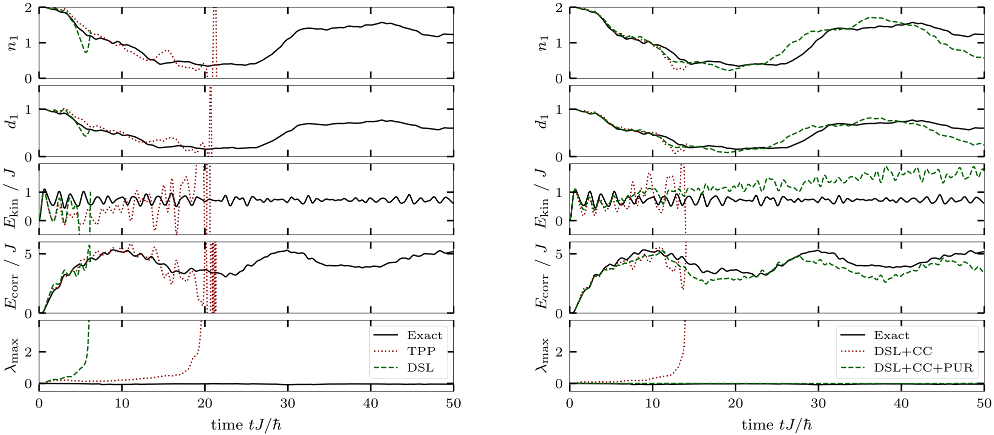

Figure 2: G1–G2 without (left) and with (right) contraction consistency (CC) and purification (PUR). Half-filled 6-site Hubbard system at moderate coupling, $U/J = 4$. Sites 1–3 are initially doubly occupied and sites 4–6 are empty. At time $t = 0$ the confinement potential is removed (quench).

[12] J-P. Joost, N. Schlünzen, H. Ohldag, M. Bonitz, F. Lackner, and I. Brezinova, PRB (2022)

G1–G2 scheme: Benchmarks against DMRG, 20 electrons[13]

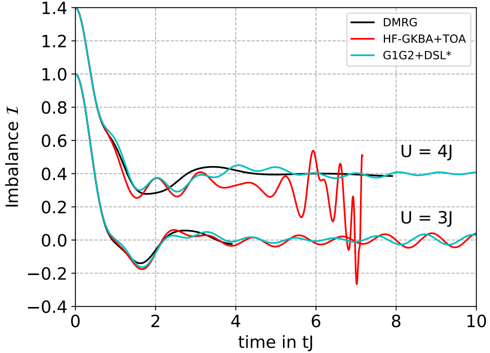

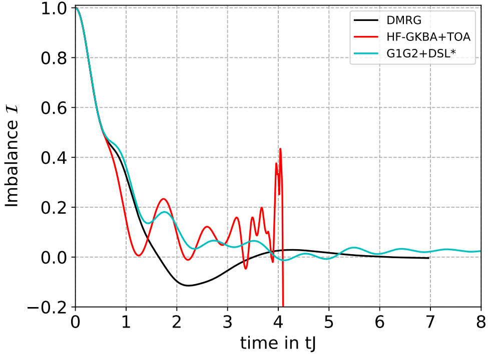

Figure 3: Relaxation of the charge Imbalance starting from a charge density wave state, $L = N = 20$ for $U/J = 3, 4$ (left) and $U/J = 5$ (right). DMRG and third order approximation (TOA) vs. G1-G2-DSL with CC and purification.

[13] J-P. Joost, N. Schlünzen, H. Ohldag, M. Bonitz, F. Lackner, and I. Brezinova, PRB (2022), DMRG and TOA data from Schluenzen et al. PRB (2017)

Motivation:

1. Prediction of petahertz electronics, sub-fs space-resolved dynamics required
2. space dependent local density of states[14], site selective laser excitation and dynamics

[14] J.-P. Joost, A.-P. Jauho, and M. Bonitz, Nano Letters **19**, 9045 (2019)

Predicted laser driven Petahertz electronics[15]

Christian-Albrechts-Universität zu Kiel
Mathematisch-Naturwissenschaftliche Fakultät

Experiments by P. Hommelhoff *et al.*: logic gate for lightwave electronics, variation of carrier envelope phase ϕ_{CE} of few cycle fs-laser pulse

a: momentum asymmetry $(A(t))$ creates $f_c(-k) \neq f(k)$ and net current

b: real space asymmetry $(E(t))$ of density creates net polarization

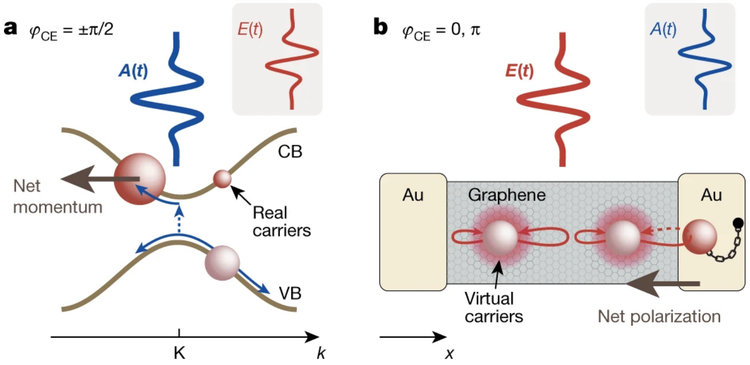

[15]Boolakee et al., Nature **605**, 251 (2022)

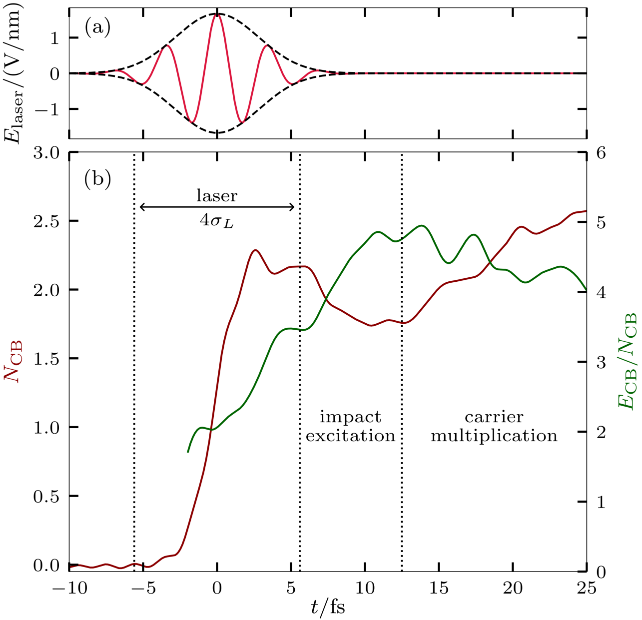

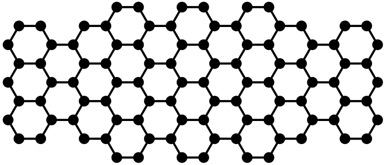

Laser parameters

- dipole approximation (wavelength μm, system nm)
- $U_{\text{pot}} = -\vec{E}_{\text{Laser}} \cdot \vec{x}$
- $E_{\text{Laser}} = E_0 \exp\left(-\frac{(t-t_0)^2}{2\sigma_L^2}\right)$
- $E_0 = 0.1$
- $\omega_L = 0.5\,J \approx 1.2\,\mathrm{eV}$
- $\sigma_L = 10\,J^{-1} \approx 3\,\mathrm{fs} \quad (\approx 0.2\,\mathrm{eV})$
- polarization: parallel to ribbon ($\|$)

Local Occupation of Excited Electrons $\parallel, E_0 = 0.1, \omega_L = 1.2\text{eV (IR)}$

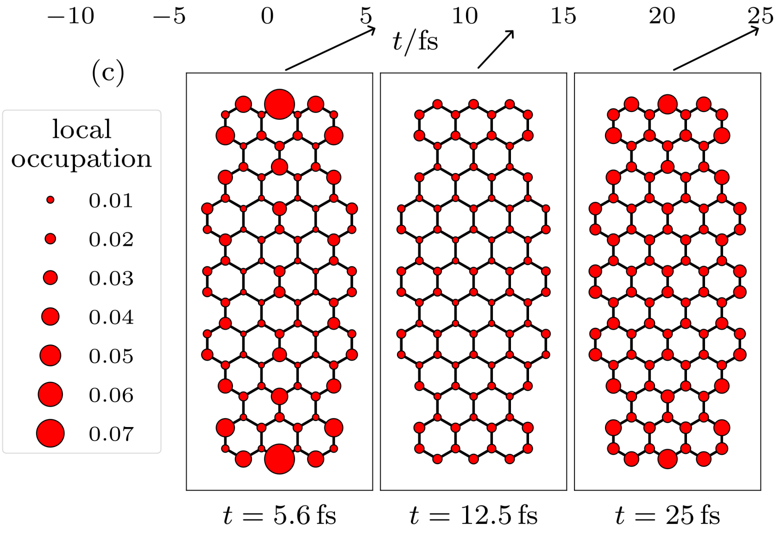

- excited electrons are first localized at the edges and subsequently redistributed

Electron spectra from G1–G2 simulations, $U/J = 4, N_B = 6$, 1D

- HF-GKBA reproduces Hartree-Fock retarded Green function, $G^R(t - t')$
- use Koopmans' theorem (ground state results)

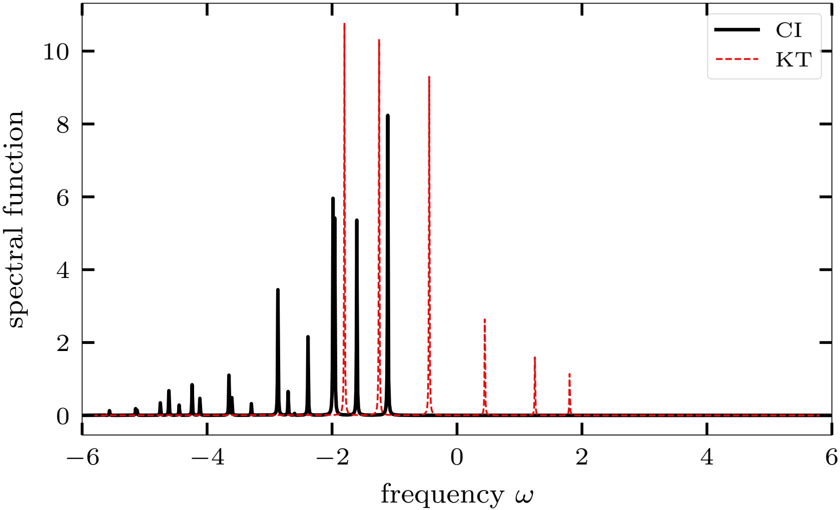

Electron spectra from G1–G2 simulations, $U/J = 4, N_B = 6$, 1D

- HF-GKBA reproduces Hartree-Fock retarded Green function, $G^R(t-t')$
- use Extended Koopmans' theorem (ground state results)

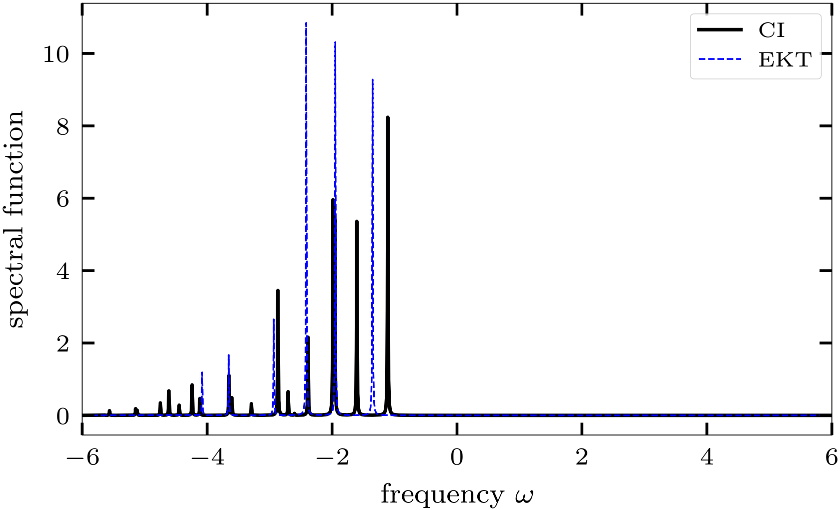

Dispersion relation from G1–G2 simulations, $U/J = 4, N_B = 54$, 1D

Christian-Albrechts-Universität zu Kiel
Mathematisch-Naturwissenschaftliche Fakultät

- HF-GKBA reproduces Hartree-Fock retarded Green function, $G^R(t - t')$
- Koopmans vs. Extended Koopmans' theorem (SOA vs. DSL), white: Bethe ansatz

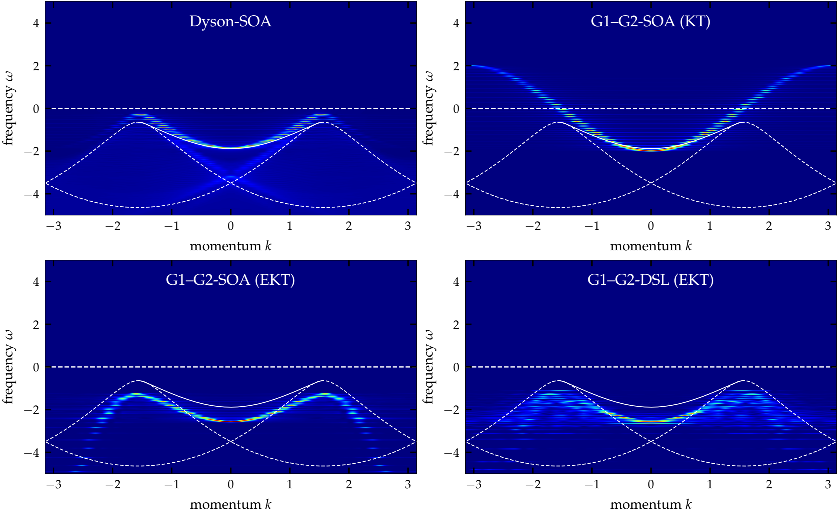

Summary and Outlook

$$\text{Full NEGF} \xrightarrow{\textbf{approximation}} \text{HF-GKBA}$$

$$\mathcal{O}(N_\mathrm{t}^3) \qquad\qquad \mathcal{O}(N_\mathrm{t}^2)$$

- HF-GKBA recovers Boltzmann-type kinetic equations and overcomes their problems: total energy conservation, correct short-time dynamics, correlated equilibrium state

Summary and Outlook

C | A | U
Christian-Albrechts-Universität zu Kiel
Mathematisch-Naturwissenschaftliche Fakultät

approximation | **no approximation!**

Full NEGF $\longrightarrow$ HF-GKBA $\longrightarrow$ G1–G2

$\mathcal{O}(N_\mathrm{t}^3)$ | $\mathcal{O}(N_\mathrm{t}^2)$ | $\mathcal{O}(N_\mathrm{t}^1)$

- HF-GKBA recovers Boltzmann-type kinetic equations and overcomes their problems: total energy conservation, correct short-time dynamics, correlated equilibrium state
- G1–G2 calculations can be done in linear time[16]
- in most cases this results in significant speed-ups ($\times 10^2$–10^4, despite rank-4 $\mathcal{G}$)
- Full nonequilibrium DSL (combining dyn. screening and strong coupling) simulations possible
- **Price to pay:** expensive storage of $\mathcal{G}_{ijkl}(t) \to$ alternative representations of interest, e.g. quantum fluctuations approach

[16] N. Schlünzen, J.-P. Joost and M. Bonitz, Phys. Rev. Lett. **124**, 076601 (2020)
J.-P. Joost, N. Schlünzen, and M. Bonitz, Phys. Rev. B **101**, 245101 (2020)
J.-P. Joost, N. Schlünzen, H. Ohldag, M. Bonitz, F. Lackner, and I. Brezinova, Phys. Rev. B **105**, 165155 (2022)

G1–G2 scheme for quasi-1D uniform dense quantum plasma

- Uniform system: use momentum representation
- radial confinement, e.g. due to magnetic field, $a^2 = 2\hbar/m\omega_c, \quad \hbar\omega_c \gtrsim k_B T$,

$$\langle \mathbf{r}\alpha' | \mathbf{k}\alpha \rangle = \frac{1}{\sqrt{L}} \left(\frac{2}{\pi a^2} \right)^{\frac{1}{2}} \exp\left(-\frac{r_\perp^2}{a^2} \right) \exp\left(\mathrm{i} r_\parallel \cdot k \right) \delta_{\alpha\alpha'},$$

- matrix element of pair potential (static screening):

$$V_{\alpha\beta}(q) = e_\alpha e_\beta \left\langle \mathbf{k}-\mathbf{q}; \mathbf{p}+\mathbf{q} \left| \frac{e^{-\kappa r}}{r} \right| \mathbf{k}; \mathbf{p} \right\rangle = e_\alpha e_\beta \exp\left[(q^2+\kappa^2)a^2 \right] \mathrm{Ei}\left[-(q^2+\kappa^2)a^2 \right],$$

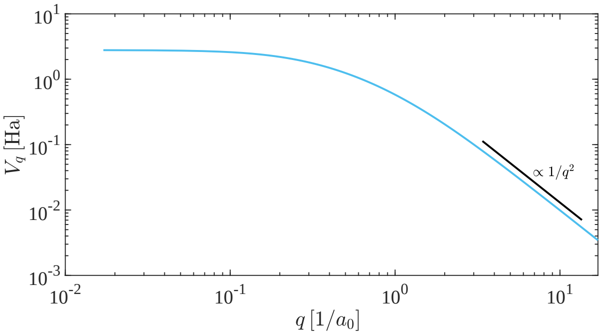

Evolution of distribution functions for fixed ion beam momentum

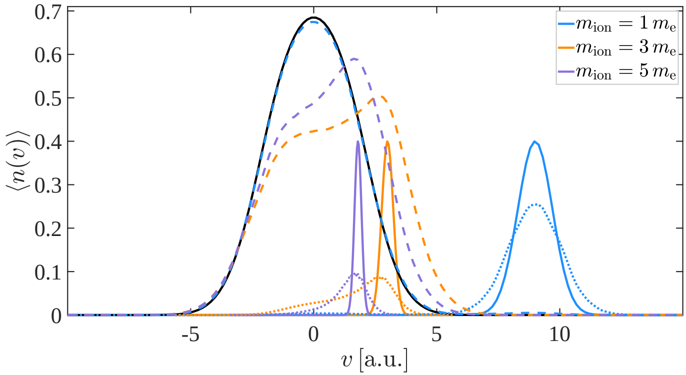

- strong (non-perturbative) beam-plasma interaction
- effective scattering in 1D only near resonance ("on shell"): $v_1 \approx v_2$
- mass-dependent scaling of peak position and width, fixed beam temperature
- existence of nonequilibrium stationary state: $F_e(v) = g \cdot F_i(v)$

[16] F. Borges-Fajardo, Bachelor thesis, Kiel University 2021, to be published

Quantum Kinetic equation for dense 3D plasmas with GKBA[17]

- spatially uniform system: use momentum representation
- But: time-local G1–G2 scheme too expensive in 2D and 3D, use standard GKBA ($\sim N_T^2$):

$$i\hbar \frac{\mathrm{d}}{\mathrm{d}t} G^{\gtrless}_{\sigma}(\mathbf{p}, tt) = 2\mathfrak{Re}\left\{ \int_{t_0}^{t} \mathrm{d}\bar{t}\, \left[\Sigma^{>}_{\sigma}(\mathbf{p}, t\bar{t}) G^{<}_{\sigma}(\mathbf{p}, \bar{t}t) - \Sigma^{<}_{\sigma}(\mathbf{p}, t\bar{t}) G^{>}_{\sigma}(\mathbf{p}, \bar{t}t) \right] \right\}$$

- GKBA: express off-diagonal G through time-diagonal G at earlier time:

$$G^{\gtrless}_{\sigma}(\mathbf{p}, t_1 t_2) = -i\hbar \left[G^{\mathcal{R}}_{\sigma}(\mathbf{p}, t_1 t_2) G^{\gtrless}_{\sigma}(\mathbf{p}, t_2 t_2) - G^{\gtrless}_{\sigma}(\mathbf{p}, t_1 t_1) G^{\mathcal{A}}_{\sigma}(\mathbf{p}, t_1 t_2) \right]$$

- HF-GKBA: Approximate $G^{\mathcal{R}/\mathcal{A}}$ on Hartree–Fock level:

$$G^{\mathcal{R}/\mathcal{A},\mathrm{HF}}_{\sigma}(\mathbf{p}, t_1 t_2) = \pm \frac{1}{i\hbar} \Theta\left(\pm(t_1 - t_2)\right) \exp\left\{ \frac{1}{i\hbar} \int_{t_2}^{t_1} \mathrm{d}\bar{t}\, h^{\mathrm{HF}}_{\sigma}(\mathbf{p}\bar{t}) \right\} .$$

- Conserves particle number, momentum, total energy, ...

---

[16] M. Bonitz, *Quantum Kinetic Theory*, 2nd ed. Springer 2016; C. Makait, Masters Thesis, CAU Kiel (2022), to be published

[17] P. Lipavský, V. Špička, B. Velický, Phys. Rev. B 1986, 34, 6933–6942

$$i\hbar \frac{\mathrm{d}}{\mathrm{d}t} G^{\gtrless}_{\mathbf{k}\alpha}(tt) = \left[I + I^{\dagger}\right]_{\mathbf{k}\alpha}(t)\,, \qquad I_{\mathbf{k}\alpha}(t) = \int_{t_0}^{t} \left\{\Sigma^{>}_{\mathbf{k}\alpha}(t\bar{t}) G^{<}_{\mathbf{k}\alpha}(\bar{t}t) - \Sigma^{<}_{\mathbf{k}\alpha}(t\bar{t}) G^{>}_{\mathbf{k}\alpha}(\bar{t}t)\right\} \mathrm{d}\bar{t}$$

$$\Sigma^{\gtrless}_{\mathbf{k}\alpha}(t_1t_2) = i\hbar Z_\alpha^2 \sum_{\mathbf{k}'} W^{\gtrless}_{\mathbf{k}'-\mathbf{k}}(t_1t_2) G^{\gtrless}_{\mathbf{k}'\alpha}(t_1t_2)$$

$$W^{\gtrless}_{\mathbf{q}}(t_1t_2) = \pi^{\gtrless}_{\mathbf{q}}(t_1t_2) w_{\mathbf{q}}(t_1) w_{\mathbf{q}}(t_2) + w_{\mathbf{q}}(t_1) \int_{t_0}^{t_1} \pi^{\mathcal{R}}_{\mathbf{q}}(t_1\bar{t}) W^{\gtrless}_{\mathbf{q}}(\bar{t}t_2)\ \mathrm{d}\bar{t} + w_{\mathbf{q}}(t_1) \int_{t_0}^{t_2} \pi^{\gtrless}_{\mathbf{q}}(t_1\bar{t}) W^{\mathcal{A}}_{\mathbf{q}}(\bar{t}t_2)\ \mathrm{d}\bar{t}$$

$$\pi^{\gtrless}_{\mathbf{q}}(t_1t_2) = i\hbar \sum_{\mathbf{k}'\beta} (\pm)_\beta Z_\beta^2 G^{\gtrless}_{\mathbf{k}'+\mathbf{q},\beta}(t_1t_2) G^{\lessgtr}_{\mathbf{k}',\beta}(t_2t_1)$$

$$k^{\mathcal{R}/\mathcal{A}}(t_1t_2) = \pm\Theta\left(\pm(t_1 - t_2)\right) \left[k^{>}(t_1t_2) - k^{<}(t_1t_2)\right]\,, \qquad k \in \{G, W, \pi, ..\}$$

- α, β: combined indices for spin and particle species, Z_α: charge number
- dynamically screened potential: $W^{\mathcal{R}}_{\mathbf{q}}(t_1t_2) = w_{\mathbf{q}}(t_1)\epsilon^{\mathcal{R}\,-1}_{\mathbf{q}}(t_1t_2)$
- Nonequilibrium plasmon mode occupation dynamics described by $W^{<}$
- singular part of $W^{\gtrless}$ included in HF hamiltonian

Stopping power test: beam as weak perturbation

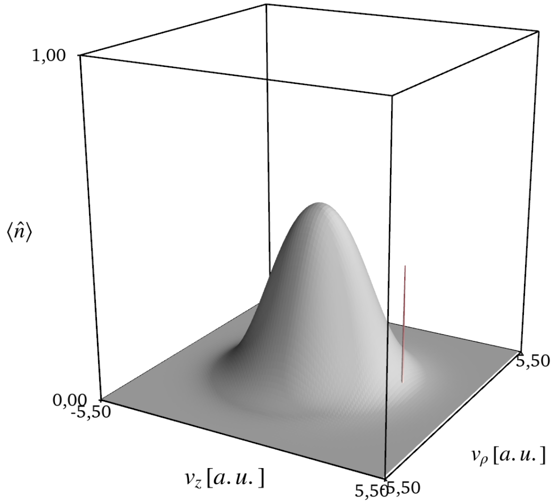

- System: spatially uniform, cylinder symmetric in momentum space (axes ρ, z)

1. For given r_s, Θ solve HF-equations,

$$h^{\text{HF}}_{\mathbf{p}\sigma} \leftrightarrow f_{\mathbf{p}} = \left[1 + \exp\beta\left(h^{\text{HF}}_{\mathbf{p}\sigma} - \mu\right)\right]^{-1}.$$

2. Start propagation after adiabatic switch on of interaction in plasma
3. Add projectile distribution: monochromatic, density $\sim 10^{-12}$ of target density
4. Propagate and find time dependent stopping power

Stopping power: $$\frac{\mathrm{d}E_{\text{kin}}}{\mathrm{d}x}(\mathbf{v}_p, t) = \pm i\hbar\frac{1}{n}\sum_\sigma\int\frac{\mathrm{d}\tilde{\mathbf{p}}}{(2\pi\hbar)^3}\frac{\tilde{\mathbf{p}}\cdot\mathbf{v}_p}{v_p}\frac{\mathrm{d}}{\mathrm{d}t}G^<_{\tilde{\mathbf{p}}+\langle\mathbf{p}\rangle,\sigma}(t,t)$$

Non-Markovian GW stopping curve[18]

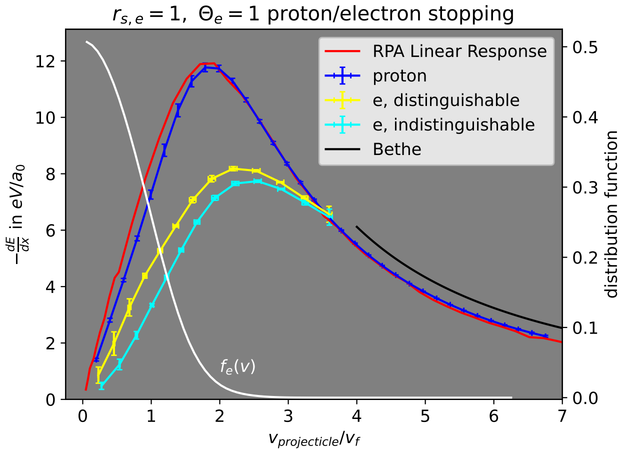

- proton stopping agrees well with RPA linear response data
- electron stopping power reduced due to Pauli blocking
- 'e, indistinguishable': electron projectiles including full antisymmetry with target

RPA data: Moldabekov, Zh., Dornheim, T., Bonitz, M. and Ramazanov, T. S., *Phys. Rev. E* **101** 053203 (2020)

[18] C. Makait, Masters Thesis, CAU Kiel (2022), to be published

Nonequilibrium Plasmon spectral function[19]

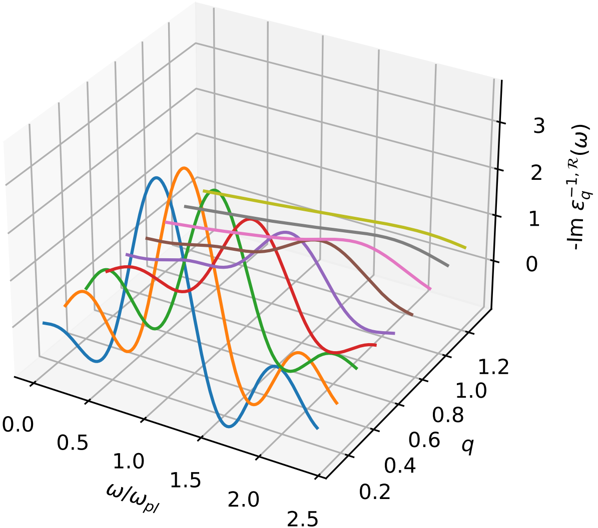

[19] C. Makait, Masters Thesis, CAU Kiel (2022), to be published

Time-dependent Plasmon mode occupation $N_{\mathrm{q}}(t) = i\hbar W^{<}_{\mathrm{q}}(t,t)$[20]

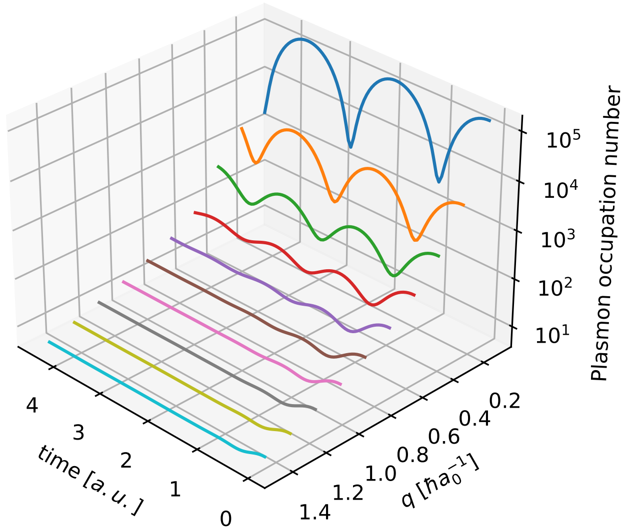

[20] C. Makait, Masters Thesis, CAU Kiel (2022), to be published

Linking short and long time scales. Multiscale concepts

C A U
Christian-Albrechts-Universität zu Kiel
Mathematisch-Naturwissenschaftliche Fakultät

- accurate NEGF (G1–G2) simulations crucial for short times to resolve electron dynamics, formation of plasmon spectrum, density of states
- For long times, this correlated all-electron dynamics is neither possible nor necessary
  $\Rightarrow$ simplified description justified
- Needed: - physically guided analysis of time and length scales, dominant modes etc.
  - systematic mathematical approach to select those modes

G1–G2 scheme: achieving long simulation times for correlated electrons: contraction consistency and purification

- Enforcing Contraction consistency[21]:

$$\frac{N}{2} G_{ij}^{\uparrow\uparrow} = -\mathrm{i}\hbar \sum_p G_{ipjp}^{(2),\uparrow\downarrow\uparrow\downarrow}$$

$$G_{ij}^{\uparrow\uparrow} = -\mathrm{i}\hbar \sum_p G_{ippj}^{(2),\uparrow\downarrow\uparrow\downarrow}$$

$$\left(\frac{N}{2} - 1\right) G_{ijkl}^{(2),\uparrow\downarrow\uparrow\downarrow} = -\mathrm{i}\hbar \sum_p G_{ipjkpl}^{(3),\uparrow\uparrow\downarrow\uparrow\uparrow\downarrow}$$

$$\frac{N}{2} G_{ijkl}^{(2),\uparrow\uparrow\uparrow\uparrow} = -\mathrm{i}\hbar \sum_p G_{ijpklp}^{(3),\uparrow\uparrow\downarrow\uparrow\uparrow\downarrow}$$

$$G_{ijkl}^{(2),\uparrow\uparrow\uparrow\uparrow} = -\mathrm{i}\hbar \sum_p G_{ipjklp}^{(3),\uparrow\uparrow\downarrow\uparrow\uparrow\downarrow}$$

$$G_{ijkl}^{(2),\uparrow\uparrow\uparrow\uparrow} = -\mathrm{i}\hbar \sum_p G_{ijpkpl}^{(3),\uparrow\uparrow\downarrow\uparrow\uparrow\downarrow}$$

[21] see e.g. papers by Coleman, Maziotti and others
F. Lackner *et al.*, Phys. Rev. A (2015), Phys. Rev. A (2017)
J-P. Joost, N. Schlünzen, H. Ohldag, M. Bonitz, F. Lackner, and I. Brezinova, PRB (2022)

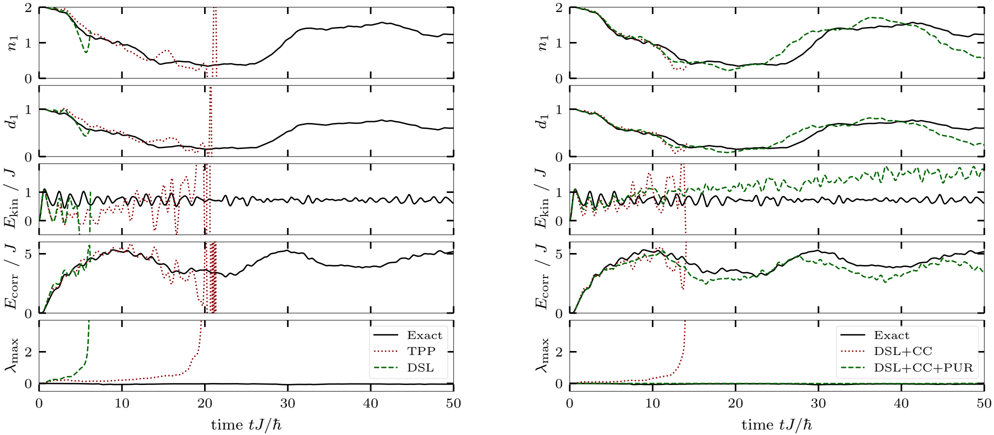

Figure 4: G1–G2 without (left) and with (right) contraction consistency (CC) and purification (PUR). Half-filled 6-site Hubbard system at moderate coupling, $U/J = 4$. Sites 1–3 are initially doubly occupied and sites 4–6 are empty. At time $t = 0$ the confinement potential is removed (quench).

[22] J-P. Joost, N. Schlünzen, H. Ohldag, M. Bonitz, F. Lackner, and I. Brezinova, PRB (2022)

G1–G2 scheme: Benchmarks against DMRG, 20 electrons[23]

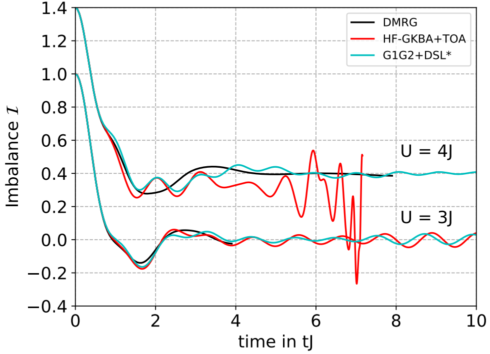

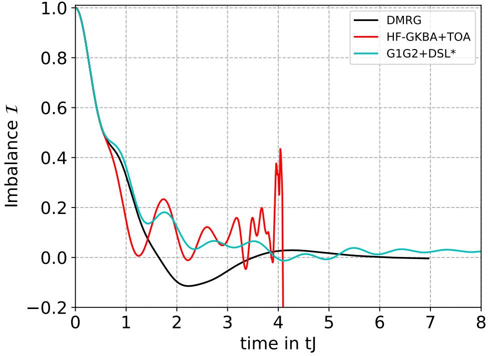

Figure 5: Relaxation of the charge Imbalance starting from a charge density wave state, $L = N = 20$ for $U/J = 3, 4$ (left) and $U/J = 5$ (right). DMRG and third order approximation (TOA) vs. G1-G2-DSL with CC and purification.

[23] J-P. Joost, N. Schlünzen, H. Ohldag, M. Bonitz, F. Lackner, and I. Brezinova, PRB (2022), DMRG and TOA data from Schluenzen et al. PRB (2017)